

**Effect of gadolinium adatoms on the transport properties of graphene**M. Alemani,<sup>1,\*</sup> A. Barfuss,<sup>1</sup> B. Geng,<sup>1</sup> C. Girit,<sup>1,†</sup> P. Reisenauer,<sup>1</sup> M. F. Crommie,<sup>1,2</sup> F. Wang,<sup>1,2</sup> A. Zettl,<sup>1,2</sup> and F. Hellman<sup>1,2</sup><sup>1</sup>*Department of Physics, University of California, Berkeley, Berkeley, California, 94720, USA*<sup>2</sup>*Materials Science Division, Lawrence Berkeley National Laboratory, Berkeley, California 94720, USA*

(Received 20 April 2012; published 14 August 2012)

The electrical transport properties of graphene doped with gadolinium (Gd) adatoms have been measured. The gate voltage dependence of the conductivity shows that Gd produces  $n$  doping of graphene. The charged Gd ions act as scattering centers, lowering the sample mobility for both electrons and holes. The doping efficiency of Gd at 77 K reproduces theoretical predictions (0.7 electron per Gd adatom). On raising the sample temperature to even 150 K, clustering effects are observed and substantially modify the transport.

DOI: [10.1103/PhysRevB.86.075433](https://doi.org/10.1103/PhysRevB.86.075433)

PACS number(s): 72.80.Vp, 73.22.Pr, 73.63.-b, 72.10.Fk

**I. INTRODUCTION**

Graphene, a single atomic layer of hexagonally coordinated carbon, has been found to exhibit exciting physical properties<sup>1</sup> that are promising for future application in electronics. Among these properties are an extremely high electronic mobility, long mean free path, and spin scattering time at room temperature.<sup>2,3</sup>

Recently, the modification of graphene electronic and magnetic properties via adsorption of chemical impurities has been a topic of great interest, as it is a central issue to understand electron mobility and correlated electron physics,<sup>4,5</sup> with applications for chemical sensors.<sup>6</sup> Charge transfer between adatoms and graphene shifts the chemical potential of graphene and modifies the charged impurity scattering.<sup>7,8</sup> By contrast, chemical reaction of hydrogen with graphene<sup>9</sup> opens a band gap, a useful characteristic for graphene to become a versatile electronic device material.

Among possible adsorbates, rare-earth atoms and Gd in particular are interesting and unexplored candidates. In contrast to most of the simple and transition metals, Gd has a large local moment, which is preserved in nearly all environments. Moreover, in addition to the large core moment magnetic moments of outer orbitals ( $6s, 5p, 5d$ ) are shown to be enhanced upon adsorption on graphene.<sup>10-13</sup> The interaction between large magnetic moments and graphene's electrons could lead to interesting correlated electron phenomena influencing the electrical properties of graphene.

In this work, we have studied the effect on graphene electrical transport of dilute quantities of gadolinium (Gd). Gd ( $4f^7 5d^1 6s^2$ ) is a rare-earth characterized by a large magnetic moment, due to its half filled  $f$  shell. Gd on graphene has been recently studied theoretically<sup>10</sup> and with a scanning tunneling microscope,<sup>14</sup> but there are no experimental studies on electrical transport.

**II. EXPERIMENTAL**

Graphene samples were prepared by chemical vapor deposition (CVD) on 25- $\mu$ m thick copper foil and then transferred onto 285 nm SiO<sub>2</sub> on top of heavily doped Si (Si<sup>++</sup>) substrates, with the use of a process similar to that described in Refs. 15 and 16. We used polystyrene and PMMA as the assisted films. In this paper, we report on two samples. Sample 1 was prepared using polystyrene as assist film, while sample 2 used PMMA. After the graphene

transfer, sample 1 was cleaned with chloroform to dissolve resist residues,<sup>17</sup> while the PMMA membrane of sample 2 was dissolved carefully with a slow acetone flow. An optical microscope image of a device is shown in Fig. 1(a). Au/Cr leads (Cr = 30 nm and Au = 200 nm) were predeposited (before the graphene transfer) on the SiO<sub>2</sub>/Si<sup>++</sup> using standard photolithography techniques. The graphene was patterned using photolithography and oxygen plasma etching. Electrical leads were wire bonded to the Au/Cr contacts and the sample mounted onto the cryostat stage of a high vacuum system with thermal evaporation sources. The resistance of the graphene was measured *in situ* before and after doping with a four-probe technique, using dc voltage. From the measured resistance  $R$ , knowing the sample geometry, we calculated the conductivity  $\sigma = 1/R \times (L/W)$ , where  $L$  and  $W$  are sample length and width. The gate-voltage-dependent conductivity  $\sigma(V_g)$  was measured by applying the gate voltage  $V_g$  to the heavily doped Si substrate.

Micro-Raman spectroscopy was used to evaluate the quality and the number of layers of the graphene films on the SiO<sub>2</sub>/Si substrates. Figure 1(b) shows the Raman spectrum of a graphene device; the shape of the peak near 2700 cm<sup>-1</sup> indicates a monolayer of graphene. Atomic force microscopy was used to measure adsorbates and thereby to verify the quality of the sample. Samples were annealed in high vacuum at 400 K for four hours to remove surface adsorbates. Before this cleaning procedure, samples were found to be strongly  $p$  doped (the gate voltages of minimum conductivity  $V_{g,\min}$  were at positive voltages) and hysteretic behavior was seen in the  $\sigma(V_g)$  curves. After the cleaning and thermal treatment, the position of  $V_{g,\min}$  was found to be close to zero gate voltages and the hysteretic behavior disappeared.

Gd was deposited *in situ* onto the graphene using thermal deposition from a tungsten basket. The source was degassed before beginning deposition onto graphene. Deposition time was controlled using a shutter and the deposition rate was measured with a crystal monitor whose tooling factor was previously calibrated. A liquid nitrogen cooled shroud surrounded the sources and cryostat, reducing the background pressure and eliminating water vapor. The base pressure during deposition was in the low 10<sup>-9</sup> Torr range.

Figure 2 shows the conductivity versus gate voltage for the pristine device and at three different Gd doping concentrations for Gd deposited and measured at 77 K. The  $\sigma$  versus  $V_g$  curves shift to negative gate voltages with increasing Gd adsorption.

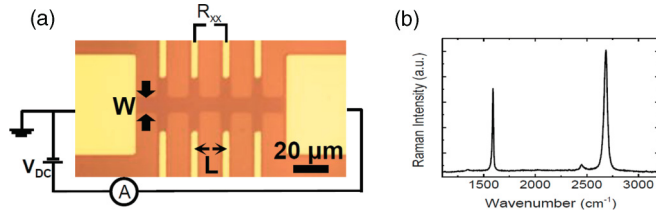


FIG. 1. (Color online) (a) Optical image of a graphene device. The graphene (dark orange area) is contacted by Au/Cr electrodes (shown in yellow). The longitudinal  $R_{xx}$  resistance is measured with a four-probe setup by applying dc voltage and measuring  $V_{xx}$ . The length  $L$  and width  $W$  of the sample are used to calculate the resistance per square  $R_{\square}$  and from that, the conductivity  $\sigma$  as  $R_{\square} = (W/L)R_{xx} = 1/\sigma$ . A back-gate voltage is applied to the underlying  $\text{Si}^{++}$  substrate. (b) Raman spectrum of the pristine graphene. The single peak near  $2700 \text{ cm}^{-1}$  is characteristic of a single-layer graphene. The small  $D$  peak at about  $1350 \text{ cm}^{-1}$  indicates no significant intervalley scattering and signifies low disorder.

The negative shift of the gate voltage  $V_{g,\text{min}}$ , at which the minimum conductivity  $\sigma_{\text{min}}$  occurs, indicates that electrons are donated to the graphene ( $n$ -type doping) and the Fermi level of graphene is driven away from the Dirac point. This is in agreement with theoretical calculations in Ref. 10, which show  $n$ -type doping for Gd on graphene. Moreover, on Gd doping sample mobility decreases,  $\sigma(V_g)$  becomes more linear, and  $\sigma_{\text{min}}$  increases, similarly to what has been observed for potassium<sup>7</sup> and transition metal atoms.<sup>8</sup>

It is important to note that after adsorption of Gd at 77 K,  $\sigma(V_g)$  curves show no time dependence within the time resolution [time for a single  $\sigma(V_g)$  measure was about six minutes]. This is in contrast to  $\sigma(V_g)$  curves for Gd adsorbed at room temperature (see discussion below).

Figure 2(b) shows the shift of the voltage of minimum conductivity  $\Delta V_{g,\text{min}}$  versus the number of Gd atoms adsorbed per area  $n_{\text{imp}}$ , for two distinct graphene devices, referred to as samples 1 and 2.  $n_{\text{imp}}$  has been extracted from the deposition rate and time and  $V_{g,\text{min}}$  is determined by the crossing of the high-voltage linear fits that are used to determine the electron and hole mobilities (see discussion below on mobility). Using  $\Delta V_{g,\text{min}}$ , we have calculated the doping efficiency  $\eta$  (i.e., the number of electrons donated to graphene per Gd atom) [see Fig. 2(c)].  $\eta$  is the ratio between the added charge carriers  $\Delta n$  and  $n_{\text{imp}}$ , where  $\Delta n = c_g \Delta V_{g,\text{min}}$  and  $c_g$  is the calculated gate capacitance per unit area equal to  $7.6 \times 10^{10} \text{ V}^{-1} \text{ cm}^{-2}$ , based on the known thickness of the oxide underlayer.

Data in Fig. 2(b) in the low doping regime ( $n_{\text{imp}} < 3 \times 10^{12} \text{ cm}^{-2}$ ) follow a linear relationship. From a linear fit  $\eta$  is calculated to be 0.7, in accordance to theoretical calculations.<sup>10</sup> The theoretical prediction is shown in Fig. 2(b) as the dashed line. Data for sample 2 in the large doping regime show a change in slope, indicating reduced doping efficiency  $\eta$  at high doping. These data show that  $\eta$  for sample 1 does not depend on  $n_{\text{imp}}$ , while for sample 2  $\eta$  decreases for larger  $n_{\text{imp}}$ .

This difference in how  $\eta$  depends on  $n_{\text{imp}}$  is likely due to the different preparation methods for the two samples. In addition to the difference in doping efficiency, an asymmetry in the mobility of electrons and holes was observed for pristine (undoped) sample 2, which was not seen for pristine sample 1.

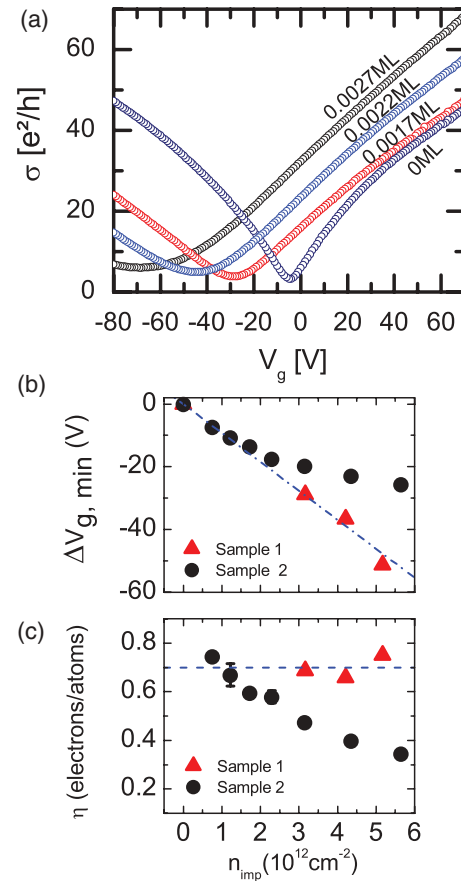


FIG. 2. (Color online) (a) Conductivity  $\sigma$  versus gate voltage  $V_g$  for pristine graphene and three coverages of Gd (the data shown are for sample 1). The graphene was held at 77 K during Gd deposition and measurements. The Gd coverage is expressed in monolayers (MLs), where 1 ML is defined as  $1.908 \times 10^{15} \text{ atoms/cm}^2$ , the areal density of a primitive unit cell of graphene. (b) Shift of the gate voltage of minimum conductivity  $V_{g,\text{min}}$  upon adsorption of Gd versus density of Gd atoms deposited ( $n_{\text{imp}}$ ) for two different graphene devices. The dashed line shows the linear relationship  $\Delta V_{g,\text{min}} = n_{\text{imp}}\eta/c_g$ , where  $c_g$  is the calculated gate capacitance per unit area and  $\eta$  (= number of electrons per Gd atom) was assumed equal to 0.7, based on theoretical calculations (Ref. 10). (c) Doping efficiency  $\eta$  versus  $n_{\text{imp}}$  for two different graphene devices. The dashed line indicates the theoretical prediction. Samples 1 and 2 were prepared by different transfer methods, and showed different  $\sigma$  vs  $V_g$  data; sample 1 is more symmetric (electron/hole mobility) and  $V_{g,\text{min}}$  occurs closer to 0 for the pristine (undoped) sample, indications of better graphene sample quality.

Asymmetries in hole and electron mobilities have been shown to be related to extrinsic effects such as the influence of metallic contacts<sup>18</sup> and doping adsorbates;<sup>19</sup> the latter is likely to be the reason of the decrease of doping efficiency seen for sample 2.

The values of  $\eta$  for sample 1 and low  $n_{\text{imp}}$  of sample 2 are in agreement with calculations of the charge transfer of isolated Gd atoms on graphene, which indicate 0.7 electrons per Gd atom.<sup>10</sup> This charge transfer results in positively charged Gd atoms on the surface of graphene, which shift the Fermi energy of the graphene (as measured by the shift of  $V_{g,\text{min}}$ ) and are also expected to act as scattering centers for the graphene charge carriers, lowering the sample mobility.

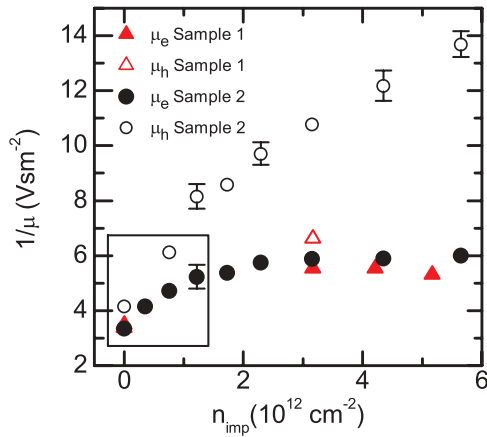


FIG. 3. (Color online) Inverse of electron and hole mobility versus number of Gd atoms deposited per area. The square indicates the range of  $n_{\text{imp}}$  used to extract the proportionality constant  $C$  to compare with theory. From the fit,  $C = \mu n_{\text{imp}} = 5.9 \times 10^{15} \text{ V}^{-1} \text{ s}^{-1}$ . Hole and electron mobilities are very similar when the mobilities of the pristine sample are similar (sample 1), while they differ if the initial mobilities are different (sample 2).

We have analyzed how the mobility of the sample changes with Gd adsorption. Hole and electron mobilities were determined by taking the slope of the  $\sigma(V_g)$  curves away from  $V_{g,\text{min}}$ , using the steepest regime of the  $\sigma(V_g)$  curves [determined by taking the derivative of  $\sigma(V_g)$ ]. Fits were carried out over a 2-V interval in  $V_g$ . The errors in the hole and electron mobilities were determined from the standard deviation of the fits. The results are shown in Fig. 3 and show that mobility decreases with increasing Gd. The relation between mobility and  $n_{\text{imp}}$  is not linear. A linear dependence  $1/\mu \propto n_{\text{imp}}$  is expected for charge impurity scattering from uncorrelated scatterers<sup>20</sup> and was observed experimentally for other atomic species.<sup>7,21</sup> To compare with theory, we have extracted the proportionality constant  $C = \mu n_{\text{imp}} = 5.9 \times 10^{15} \text{ V}^{-1} \text{ s}^{-1}$  from a linear fit of electron mobilities for small  $n_{\text{imp}}$  (indicated by the square). This is in good agreement with the theory of pointlike charge impurity scattering by Hwang *et al.*,  $C = 5 \times 10^{15} \text{ V}^{-1} \text{ s}^{-1}$ .<sup>22</sup>

The electron mobility for larger  $n_{\text{imp}}$  saturates. Similar effects have been observed in other experiments,<sup>8,21</sup> but the origin is still not clear. Since it is known that the formation of large circular clusters decreases the scattering cross section with respect to that of isolated atoms,<sup>23</sup> we suggest that when more material is added, Gd clusters form and the mobility is not reduced.

By considering the full  $\sigma(V_g)$  data (see Fig. 2), the differential mobility  $d\sigma/d(V_g)$  at high charge densities seems to increase with Gd concentration. The  $\sigma(V_g)$  data for the pristine samples separate into a linear and sublinear part.<sup>24</sup> On adding Gd, the linear part of  $\sigma(V_g)$  becomes more extended in gate voltage range. Since we are limited in the applicable gate voltage, it is not possible to clearly identify the beginning of a sublinear part after Gd has been adsorbed.

We turn now to the discussion of the effect of temperature  $T$ . Following the deposition on sample 1 at 77 K, the transport properties were monitored as the temperature of the sample was increased to 300 K. Figure 4 shows the sample mobility

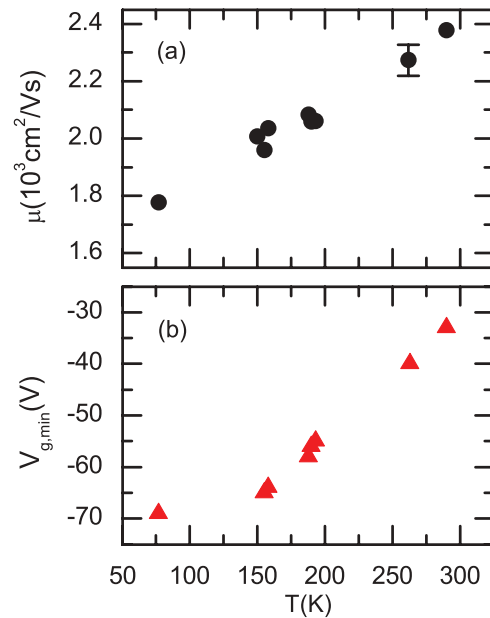


FIG. 4. (Color online) Temperature dependence of electron mobility (a) and gate voltage of minimum conductivity (b) for sample 1.

and  $V_{g,\text{min}}$  as a function of  $T$ . As  $T$  is increased,  $\mu$  increases and  $V_{g,\text{min}}$  shifts to less negative voltages. Similar effects were observed for gold atoms on graphene and have been attributed to clustering of gold adatoms.<sup>21</sup> As we have discussed before, the formation of clusters decreases the scattering cross section as compared to isolated atoms,<sup>21,23</sup> increasing the sample mobility. While the mobility increases constantly in the whole temperature range studied,  $V_{g,\text{min}}$  shifts only slightly between 77 K and 150 K, and more rapidly for higher  $T$ . The increase in  $V_{g,\text{min}}$  for  $T > 150$  K, is likely due to the reduced charge transfer per Gd atom due to the formation of larger size clusters, which act more like metallic electrodes than individual atoms.<sup>21</sup> The fact that the mobility changes over the whole temperature range is an indication that even if  $V_{g,\text{min}}$  is not influenced between 77 K and 150 K, changes in the scattering, attributed to clustering of Gd adsorbates, occur starting immediately above 77 K. These data suggest that clusters of Gd still are able to effectively dope graphene, but are less effective at scattering the resulting carriers.

After warming sample 1 to room temperature we deposited additional Gd onto it. By measuring the  $\sigma(V_g)$  curves directly after Gd doping, we observed a shift of the curves towards negative gate voltages similar to what we observed for doping at 77 K. However,  $\sigma(V_g)$  curves change with time, unlike at 77 K. The time-dependent mobility and shift of  $V_{g,\text{min}}$  are shown in Fig. 5 and are likely related to clustering of Gd, which occurs at room temperature, as can be seen in the AFM image shown in the inset of Fig. 5. Scanning tunneling microscope images for Gd deposited on graphene at room temperature<sup>10,14</sup> show the formation of fractal-like noncrystalline islands and theoretical calculations of adsorption and diffusion energies confirm mobility of Gd atoms on graphene at room temperature.<sup>10</sup> It is likely that these effects are due to clustering of Gd rather than oxidation both because of low background pressure and because oxidation of adsorbates on

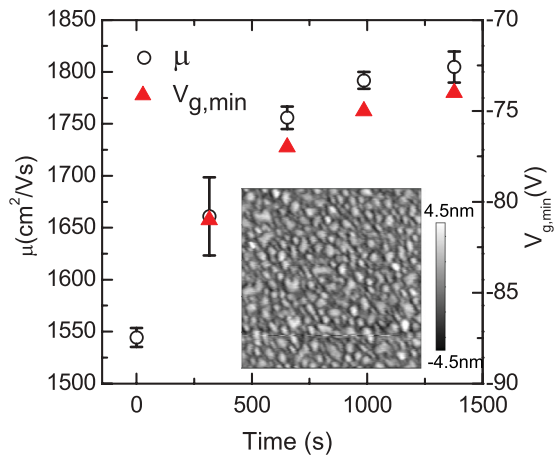


FIG. 5. (Color online) Time dependence of electron mobility (empty circles) and voltage of minimum conductivity (filled triangles) for Gd deposited at room temperature on sample 1. The amount of Gd deposited is  $n_{\text{imp}} = 2.7 \times 10^{12} \text{ cm}^{-2}$ . (Inset) AFM image ( $1 \mu\text{m} \times 1 \mu\text{m}$ ) of Gd deposited on graphene at room temperature, which exhibits isolated islands. At 77 K, no time dependence is seen.

graphene has been observed to produce much larger effects on conductivity than the present results.<sup>25</sup>

We have also done preliminary measurements of the effect of yttrium (Y) atoms deposited on graphene. Y ( $4d^1 5s^2$ ), like Gd, is a trivalent material with nearly identical ionic radius as Gd. Therefore, Y and Gd should introduce the same electronic potential disorder to the system and similar outermost electrons, hence carriers. They differ only by the presence or absence of the inner  $4f$  shell of Gd, which at least in three-dimensional (3D) semiconducting materials causes magnetic disorder, which strongly impacts electrical conduction.<sup>26</sup> By doping Y on graphene at 77 K ( $n_{\text{imp}}$  was varied from  $0.4 \times 10^{12} \text{ cm}^{-2}$  to  $60 \times 10^{12} \text{ cm}^{-2}$  in ten steps), we measured  $n$  doping of graphene, as in the case of Gd. The measured doping efficiency for Y was 0.1 electrons donated

for Y atoms, lower but of the same order of magnitude as that found for Gd. We also observed a decrease in  $\mu$  by adding Y, but the decrease in  $\mu$  was also lower for Y than Gd. This could be an indication of additional scattering mechanism related to the Gd magnetism. On the other hand, the larger impact on  $\mu$  for Gd could be related to different initial sample quality ( $\mu$  of the pristine graphene is about  $1000 \text{ cm}^2 \text{ V}^{-1} \text{ s}^{-1}$  for the Y sample and about  $3000 \text{ cm}^2 \text{ V}^{-1} \text{ s}^{-1}$  for the Gd samples). Further studies are necessary to understand if Gd adsorbates truly have a different doping efficiency and effect on mobility than Y.

### III. CONCLUSION

In conclusion we have shown that Gd adsorbates have a strong effect on the electrical transport properties of graphene. Gd produces  $n$  doping of graphene, with a doping efficiency of 0.7 electrons per Gd atom. The measured doping efficiency confirms theoretical calculations for isolated Gd atoms on graphene. At 77 K, Gd atoms act as charged pointlike scattering centers lowering the sample mobility. On raising the temperature, formation of larger clusters modifies the transport substantially, reducing the doping efficiency and the scattering.

### ACKNOWLEDGMENTS

This work was supported by NSF NIRT Grant No. ECS-0609469. We gratefully acknowledge A. Lanzara for discussions, D. Goldhaber-Gordon, K. Todd, and F. Fricke for their help and assistance in making transport measurements of graphene samples at the early stage of the experiment, and C. Baldasseroni for assistance in device preparation. A.Z. acknowledges support from the Director, Office of Energy Research, Materials Sciences and Engineering Division, of the US Department of Energy under Contract No. DE-AC02-05CH11231, which provided for graphene synthesis, and the Office of Naval Research (MURI), which provided for Raman spectroscopy.

\*alemanimicol@gmail.com

<sup>†</sup>Present Address: Quantronics Group, Service de Physique de l'État Condensé (CNRS URA 2464), IRAMIS, DSM, CEA-Saclay, 91191 Gif-sur-Yvette, France.

<sup>1</sup>K. S. Novoselov, A. K. Geim, S. V. Morozov, D. Jiang, Y. Zhang, S. V. Dubonos, I. V. Grigorieva, and A. A. Firsov, *Science* **306**, 666 (2004).

<sup>2</sup>K. S. Novoselov, A. K. Geim, S. V. Morozov, D. Jiang, M. I. Katsnelson, I. V. Grigorieva, S. V. Dubonos, and A. A. Firsov, *Nature (London)* **438**, 197 (2005).

<sup>3</sup>N. Tombros, C. Jozsa, M. Popinciuc, H. T. Jonkman, and B. J. van Wees, *Nature (London)* **448**, 571 (2007).

<sup>4</sup>B. Uchoa and A. C. Neto, *Phys. Rev. Lett.* **98**, 146801 (2007).

<sup>5</sup>B. Uchoa, V. N. Kotov, N. M. R. Peres, and A. H. Castro Neto, *Phys. Rev. Lett.* **101**, 026805 (2008).

<sup>6</sup>F. Schedin, A. Geim, S. Morozov, E. Hill, P. Blake, M. Katsnelson, and K. Novoselov, *Nature Mater.* **6**, 652 (2007).

<sup>7</sup>J. H. Chen, C. Jang, S. Adam, M. S. Fuhrer, E. D. Williams, and M. Ishigami, *Nature Phys.* **4**, 377 (2008).

<sup>8</sup>K. Pi, K. M. McCreary, W. Bao, W. Han, Y. F. Chiang, Y. Li, S.-W. Tsai, C. N. Lau, and R. K. Kawakami, *Phys. Rev. B* **80**, 075406 (2009).

<sup>9</sup>D. C. Elias, R. R. Nair, T. M. G. Mohiuddin, S. V. Morozov, P. Blake, M. P. Halsall, A. Ferrari, D. W. Boukhvalov, M. I. Katsnelson, A. K. Geim *et al.*, *Science* **323**, 610 (2009).

<sup>10</sup>X. Liu, C. Z. Wang, M. Hupalo, Y. X. Yao, M. C. Tringides, W. C. Lu, and K. M. Ho, *Phys. Rev. B* **82**, 245408 (2010).

<sup>11</sup>K. T. Chan, J. B. Neaton, and M. L. Cohen, *Phys. Rev. B* **77**, 235430 (2008).

<sup>12</sup>H. Sevincli, M. Topsakal, E. Durgun, and S. Ciraci, *Phys. Rev. B* **77**, 195434 (2008).

<sup>13</sup>I. S.-Martinez, A. Felten, J. J. Pireaux, C. Bittencourt, and C. P. Ewels, *J. Nanosci. Nanotechnol.* **9**, 6171 (2009).

<sup>14</sup>M. Hupalo, S. Binz, and M. Tringides, *J. Phys.: Condens. Matter* **23**, 045005 (2011).

- <sup>15</sup>X. Li, W. Cai, J. An, S. Kim, J. Nah, D. Yang *et al.*, *Science* **324**, 1312 (2009).
- <sup>16</sup>A. Reina, H. Son, L. Jiao, B. Fan, M. S. Dresselhaus, Z. Liu *et al.*, *J. Phys. Chem. C* **112**, 17741 (2008).
- <sup>17</sup>Z. Cheng, Q. Zhou, C. Wang, Q. Li, C. Wang, and Y. Fang, *Nano Lett.* **11**, 767 (2011).
- <sup>18</sup>B. Huard, N. Stander, J. A. Sulpizio, and D. Goldhaber-Gordon, *Phys. Rev. B* **78**, 121402 (2008).
- <sup>19</sup>D. B. Farmer, R. Golizadeh-Mojarad, V. Perebeinos, Y.-M. Lin, G. S. Tulevski, J. C. Tsang, and P. Avouris, *Nano Lett.* **9**, 388 (2008).
- <sup>20</sup>S. Adam, E. Hwang, V. Galitski, and S. D. Sarma, *Proc. Natl. Acad. Sci.* **104**, 18392 (2007).
- <sup>21</sup>K. M. McCreary, K. Pi, A. G. Swartz, W. Han, W. Bao, C. N. Lau, F. Guinea, M. I. Katsnelson, and R. K. Kawakami, *Phys. Rev. B* **81**, 115453 (2010).
- <sup>22</sup>E. Hwang, S. Adam, and S. D. Sarma, *Phys. Rev. Lett.* **98**, 186806 (2007).
- <sup>23</sup>M. I. Katsnelson, F. Guinea, and A. K. Geim, *Phys. Rev. B* **79**, 195426 (2009).
- <sup>24</sup>K. Nomura and A. H. MacDonald, *Phys. Rev. Lett.* **98**, 076602 (2007).
- <sup>25</sup>K. M. McCreary, K. Pi, and R. K. Kawakami, *Appl. Phys. Lett.* **98**, 192101 (2011).
- <sup>26</sup>F. Hellman, M. Q. Tran, A. E. Gebala, E. M. Wilcox, and R. C. Dynes, *Phys. Rev. Lett.* **77**, 4652 (1996).